Biochimica et Biophysica Acta 1848 (2015) 2779–2788

Contents lists available at ScienceDirect

Biochimica et Biophysica Acta

journal homepage: www.elsevier.com/locate/bbamem

Induction of eryptosis by low concentrations of *E. coli* alpha-hemolysin

Fernanda Carrizo Velásquez [a], Sabina Maté [a], Laura Bakás [b], Vanesa Herlax [a,*]

[a] Instituto de Investigaciones Bioquímicas de La Plata (INIBIOLP), CCT-La Plata, CONICET, Facultad de Ciencias Médicas, Universidad Nacional de La Plata, 60 y 120, 1900 La Plata, Argentina
[b] Departamento de Ciencias Biológicas, Facultad de Ciencias Exactas, Universidad Nacional de La Plata, 47 y 115, 1900 La Plata, Argentina

ARTICLE INFO

Article history:
Received 18 May 2015
Received in revised form 6 August 2015
Accepted 18 August 2015
Available online 21 August 2015

Keywords:
RTX toxin
Eryptosis
μ-Calpains
Endogenous sphingomyelinase
Cytoskeleton

ABSTRACT

Uropathogenic strains of *Escherichia coli* deliver the toxin alpha-hemolysin (HlyA) to optimize the host environment for the spread of infection. It was reported that at high concentrations, the toxin forms pores in eukaryotic membranes, leading to cell lysis, while lower concentrations have appeared to interfere with host–cell-signaling pathways causing cell death by apoptosis. Nevertheless, what is not clear is how often HlyA reaches levels that are high enough to lyse host target cells during the course of an infection. In the present investigation, we demonstrate that a low toxin concentration induces the suicidal death of erythrocytes (eryptosis), the major cell type present in blood. Eryptosis is triggered both by an increment in intracellular calcium and by ceramide. Since we have previously demonstrated that a low concentration of HlyA induces an increase in intraerythrocyte calcium, in the present experiments we have shown that this ion activates calpains, which hydrolyze skeleton proteins such as spectrin, ankyrin, protein 4.1 and the electrophoretic Band-3 species, thus resulting in morphologic changes in the erythrocytes. We furthermore observed that a low toxin concentration induced the activation of endogenous sphingomyelinases that in turn increased the amount of ceramide in erythrocyte membranes. Both spectrin proteolysis and ceramide formation may cause the exposure of phosphatidylserine on the membrane so as to trigger a macrophage engulfment of the erythrocyte. By this means eryptosis may be an advantageous mechanism for removing defective erythrocytes before hemolysis.

1. Introduction

Alpha hemolysin (HlyA)—the major virulence factor of uropathogenic *Escherichia coli* strains—causes 50% of all extraintestinal infections in humans [1,2]. During the last years, HlyA has been considered the prototype of a large family of pore-forming toxins, denoted as RTX [3,4].

The pore-forming toxins—besides their cytotoxic activity—can trigger cellular responses that may produce serious long-term effects in host organism. Many of these responses are triggered by an uncontrolled flux of calcium across the plasma membrane. The influx of this ion has been studied in several types of cells treated with HlyA [5–7]. With respect to erythrocytes treated with HlyA, Skals et al. demonstrated that the ATP leakage and Ca^{2+} influxes caused by the insertion of HlyA into membranes, activate purinergic receptors and pannexin channels [8]. This activation further potentiates the influx of extracellular Ca^{+2} and contributes to the shrinkage and crenation of erythrocytes resulting from the activation of calcium-dependent K^+ channels (Gardos channels) and the Cl^- channel TMEM16A [9]. Recently, we were able to quantify the intracellular calcium concentration of erythrocytes by fluorescence lifetime-imaging microscopy, using phasor representation [10]. We demonstrated that in rabbit erythrocytes the interaction with HlyA causes a fourfold increase in intracellular calcium before the occurrence of hemolysis.

In recent years, Skals et al. introduced the idea of how autocrine and/or paracrine signaling and the cell's intrinsic volume regulation markedly influence the fate of erythrocytes after HlyA membrane insertion [8,9,11]. For many years, erythrocytes had been thought to be simply membranous hemoglobin-containing vesicles floating in the circulation. In the last decade, studies on calcium homeostasis in erythrocytes have increased since the discovery that a small rise in intraerythrocyte calcium triggers apoptosis (eryptosis) despite the absence of organelles such as nuclei and mitochondria. The most recent studies disclosed that increased cytosolic Ca^{2+} activity and ceramide both trigger eryptosis, a process characterized by the exposure of phosphatidylserine (PS) on the erythrocyte surface. Erythrocytes with PS exposed in this manner may be engulfed by macrophages or may adhere to vascular endothelial [12].

In nucleated cells, caspases are essential mediators of apoptosis; in contrast, in erythrocytes μ-calpain is the protease responsible for inducing the cleavage of several membrane proteins to produce morphologic alterations such as cell shrinkage [13–15]. Calpains are calcium-dependent cysteine proteases that exist constitutively as inactive proenzymes. By the increment of cytosolic calcium, calpain translocates from the cytosol to the erythrocyte membrane, where it undergoes

Abbreviations: HlyA, alpha hemolysin; PS, phosphatidylserine; SMase, sphingomyelinase; PC, phosphatidylcholine; SM, sphingomyelin.

* Corresponding author at: INIBIOLP, Facultad de Ciencias Médicas, 60 y 120, 1900 La Plata, Argentina.
E-mail address: vherlax@med.unlp.edu.ar (V. Herlax).

http://dx.doi.org/10.1016/j.bbamem.2015.08.012
0005-2736/

autoproteolytic activation [16]. The targets of activated calpain are mainly transmembrane or membrane-associated proteins including the plasma-membrane Ca^{2+} pump and the proteins constituting electrophoretic bands 1 and 2 (the α and β spectrins, respectively) plus bands 2.1, 3, 4.1, and 4.2, in addition to calpain itself [17,14]. Calpastatin is the natural regulator of the enzyme's activity in erythrocytes. Its interaction with calpain is also Ca^{2+} sensitive [16].

On the basis of all these results, in the present work we studied the effect of HlyA on calpain activation and ceramide formation in erythrocytes and accordingly demonstrated that a low concentration of HlyA induces eryptosis.

2. Experimental procedures

2.1. Materials

HlyA was purified from culture filtrates of the *E. coli* strain WAM 1824 [18] that was kindly provided by Dr. R. A. Welch, University of Wisconsin, Madison, USA. Calpain inhibitor II (A6060), monoclonal anticeramide antibodies (C8104-50TST), and FITC-labeled goat anti (mouse IgG) antibodies (F2653) were purchased from Sigma Chemical Co. (MO, USA). The Ringer buffer (pH 7.4) contained (in mM): 125 NaCl, 5 KCl, 1 $MgSO_4$, 32 HEPES, 5 glucose, and 1 $CaCl_2$.

2.2. Erythrocyte preparation

Human erythrocytes were isolated from the defibrinated venous blood of healthy volunteers, who gave the appropriate informed consent. The total erythrocyte population was separated from the other blood components by centrifugation at 2000 *g* for 15 min at 20 °C. After three washings with 0.9% (w/v) NaCl by centrifugation at 2000 *g* for 5 min, the packed cells were resuspended in Alsever's solution (Sigma Chemical Co., USA) for storage at 4 °C for no more than two days.

2.3. Protein purification

E. coli HlyA was purified from culture filtrates of the overproducing strain WAM 1824. Cultures were grown in Luria–Bertani medium to late log phase to an absorbance of 0.8–1.0 at 600 nm (A_{600}), the cells pelleted, and the toxin in the supernatant concentrated and partially purified by precipitation with 20% (v/v) cold aqueous ethanol at pH 4.5, the toxin's pI. The pellet containing the toxin was collected by centrifugation (1 h, 14,500 *g* in a Sorvall centrifuge, rotor SSA 34) and then resuspended in TC buffer (20 mM Tris, 150 mM NaCl, pH 7.4) supplemented with 6 M guanidinium hydrochloride. Sodium-dodecylsulfate-polyacrylamide-gel electrophoresis (SDS-PAGE) of this preparation showed a main band at 110 kDa corresponding to more than 90% of the total protein (Supplementary Fig. S1). Small proteins were removed by molecular dialysis (membrane cutoff, 30 kDa). The resulting proteins were stored at −70 °C in guanidinium hydrochloride and were dialyzed in TC buffer (1:100 v/v) at 4 °C for 4 h before use in each experiment.

2.4. Hemolytic assays

Hemolysis was determined by measuring light scattering at 595 nm of a human erythrocyte suspension. The proteins were serially diluted in Ringer's buffer in a 96-well microtiter plate.

Of the diluted suspensions, 100 μl were mixed with 100 μl of 5% (v/v) erythrocytes in Ringer's buffer. The plate was then incubated at 37 °C for 30 min and the absorbance at 595 nm measured with a Multimode Detector DTX 880 Beckman Coulter.

The percent hemolysis was calculated at 30 min by Eq. (1):

$$\%\,\text{hemolysis} = (OD_c - OD_x) * 100/(OD_c - OD_{Tx}) \quad (1)$$

where OD_C is the optical density of the control erythrocytes, OD_x is the optical density of the erythrocytes treated with different concentrations of toxin, and OD_{Tx} is the optical density of erythrocytes after the addition of Triton X-100.

The D_{50} was defined as the amount of HlyA needed to produce a 50% lysis of the erythrocyte suspension.

2.5. Calpain activity

The calpain assay involves the hydrolysis of whole casein molecules by members of the calpain family and the subsequent detection at 280 nm of trichloroacetic-acid–soluble casein peptides [19]: 800 μl of assay buffer (100 mM Tris–acetate [pH 7.5], 100 mM KCl, 500 μM $CaCl_2$ [for μ-calpain], 5 mM dithiothreitol, 5 mg/ml casein) was added to 200 μl of cell suspension (hematocrit 5% after treatment with 3.5 and 7.0 pM HlyA for 5 and 15 min at 37 °C) and the mixture incubated for 30 min at 25 °C, followed by the addition of 800 μl of ice-cold 5% (v/v) trichloroacetic acid to stop the reaction. Then, the mixture was centrifuged at 4000 *g* for 10 min and the absorbance of the supernatant measured at 280 nm. The controls samples were prepared by mixing 800 μl of control buffer (the assay buffer with 10 mM ethylenediaminetetraacetic acid replacing the $CaCl_2$), 800 μl of ice-cold trichloroacetic acid, and 200 μl of cell suspension, sequentially without incubation. The enzyme activity was obtained by subtracting the absorbance of the control sample from that of the test samples.

2.6. Lipid-dot-blot assay

One ,microliter of each lipid was spotted onto nitrocellulose membranes (GE Healthcare) from a 1 mM stock solution in chloroform. The membranes were left to dry at room temperature for 1 h in order to evaporate all the solvent; next blocked for 2 h in TBS buffer (10 mM Tris–HCl, 150 mM NaCl, pH 7.4); then washed five times in TBS buffer, each time for 5 min; and finally incubated with mouse anticeramide antibodies in 3% (v/v) skim milk in TBS buffer (1:100) for 1 h. The membranes were then washed with TBS buffer and incubated with secondary goat antimouse antibodies conjugated with fluorescein isothiocyanate (goat antimouse IgG-FITC; 1:500) for 30 min. Finally, the membranes were washed once again with TBS buffer as above and the fluorescence measured in a STORM 840 Molecular Imager.

2.7. Determination of ceramide formation

The activation of endogenous sphingomyelinases (SMases) was determined by measuring ceramide formation in time by an immunofluorescence assay. Erythrocytes (0.1% (v/v) were incubated with 3.5 pM of HlyA at 37 °C for 2, 5, 10 and 15 min. Samples were centrifugated at 6000 rpm, the supernatant was separated to measure hemoglobin release by spectroscopy at 412 nm and erythrocytes were fixed with 1% (v/v) glutaraldehyde/Ringer buffer (20 min, 4 °C), and finally pelleted onto coverlips coated with 0.001% v/v poly-L-lysine (200 g, 5 min, 20 °C). After three washes with Ringer's buffer the cells were exposed to mouse anticeramide antibodies (1:5) followed by goat antimouse IgG-FITC (1:20). Fluorescence images were captured with an Olympus DP70 digital camera attached to an Olympus BX51 microscope with an excitation of 460–495 nm (emission filter 510–550 nm). An objective of 100× with a NA of 1.35 was used. Captured images were exported to an image analysis program (ImageJ) for their analysis.

2.8. SDS-PAGE of ghost erythrocytes treated with HlyA

Human erythrocytes (4 ml of a 5% [v/v] solution) were incubated with different concentrations of HlyA (3.5, 7.0, and 1000 pM) for 30 min at 37 °C. Then the samples were centrifuged at 14,500 *g* for 10 min and the erythrocytes osmotically lysed in 10 mM Tris–HCl,

pH 7.4 buffer, at 4 °C for 30 min. The membranes were precipitated by centrifugation during 10 min at 14,500 *g*, and washed by centrifuging in the same buffer until the supernatant remained clear. The membrane proteins were quantified by the method of Bradford [20]. Finally, 20 μg of proteins were separated by SDS-PAGE on a 5–20% (w/v) gradient gel. Proteins were stained with Coomassie blue R-250 and the band intensity quantified by means of the software Image-J.

2.9. Mass spectrometric analysis

Gel slices from bands A, B, C and D, derived from different experimental conditions: control, 7 pM and 1 nM HlyA, were in gel-digested with trypsin. Tryptic peptides were separated using an EASY-nLC 1000 LC system (Thermo Scientific). Samples were loaded at a constant flow of 300 nl/min onto an EASY-Spray Column (C18, 2 μm, 100A, 50 μm × 150 mm) (Thermo Scientific). After trap enrichment peptides were eluted with a linear gradient from 5–50% solvent B (acetonitrile with 0.1% formic acid) over 45 min with a constant flow of 300 nl/min. The EASY nLC system was coupled to an Orbitrap Q Exactive (Thermo Scientific). Full scan MS survey spectra (m/z 400–2000) in profile mode, were acquired in the Orbitrap with a resolution of 70,000 after accumulation of 3 e^6 ions. The ten most intense peptide ions from the preview scan were fragmented by Higher-Energy Collisional Dissociation (Activation type: HCD, Normalized collision energy: 27%, Isolation width: 3 m/z) after accumulation of 50,000 ions and analyzed in the Orbitrap at 7500 resolution. Maximal filling times were 100 ms for the FT-MS full scans and 120 ms for the FT-MS/MS scans.

Protein identification and quantitation was performed using Proteome Discoverer (Version 1.4.1.14) with Sequest HT database searching against the Uniprot *Homo sapiens* database. Mass tolerance for peptide precursors was set at 5 ppm with fragment mass tolerance set at 0.02 Da. Enzyme specificity was set to trypsin with a maximum of two missed cleavages. Two modifications were considered: fixed carbamidomethylation of cystein and variable oxidation of methionine. False Discovery Rate was set to 1% with a minimum of two high confidence peptides for quantitation.

2.10. Statistical analysis

A Student's *t*-test was used for statistical comparisons among groups and differences were considered statistically significant when $P < 0.05$ ($^*P < 0.05$, $^{**}P < 0.01$, $^{***}P < 0.001$).

3. Results

3.1. HlyA hemolytic activity

The purpose of the assay was to determine the toxin concentration to use in subsequent experiments, with an aim at working in sublytic concentrations. Fig. 1, Panel A shows the hemolysis kinetics of human-erythrocyte suspensions exposed to increasing molar concentrations of toxin. As expected, the hemolysis was greater and faster as the toxin levels increased. Fig. 1, Panel B indicates the percent hemolysis calculated at 30 min over a wide range of toxin concentrations. Since the HlyA concentration producing 50% erythrocyte lysis was 9.54×10^{-12} M (9.5 pM), further experiments were performed at toxin concentrations below this level. The hemolysis–kinetics curve at this toxin concentration should fall between curves a and b of Fig. 1, Panel A, which loci correspond to 1.4×10^{-11} M (14 pM) and 7×10^{-12} M (7.0 pM) of HlyA, respectively.

3.2. Ceramide formation in erythrocytes treated with HlyA

Suicidal erythrocyte death or eryptosis is characterized by cell shrinkage, membrane blebbing, and the exposure of PS on the cell surface. The signaling of eryptosis also involves activation of SMase with the formation of ceramide [21]; which sphingolipid, in combination with Ca^{2+}, stimulates cell-membrane scrambling. Ca^{2+} further activates Gardos channels, which are Ca^{2+}-sensitive K^+ channels, leading to cellular K^+ loss and cell shrinkage. Calcium also activates calpains, resulting in a degradation of the cytoskeleton [22,23]. Some of these characteristics were previously reported by Skals et al., for erythrocytes treated with sublytic concentrations of HlyA [9,11].

Since increased cytosolic-Ca^{+2} concentrations and ceramide both trigger eryptosis, we studied the formation of that sphingolipid in HlyA-treated erythrocytes by immunofluorescence. In order to ensure we were working at sublytic concentration, we followed the hemolysis process by optical microscopy during 15 min at different toxin concentration below 9.5 pM. Figs. 2 and 3, Panel A show that within the first 15 min, 3.5 pM of HlyA does not produce hemolysis, although an increased of crenated erythrocytes is observed at 2 min of toxin interaction (Fig. 3, Panel A). The volume of erythrocytes treated with HlyA, most notably, decreased, as a result of an activation of the K^+ channels by Ca^{2+}, as had been reported previously by Skals et al. [9]. The lack of hemolysis during HlyA–erythrocyte incubation is also shown in Fig. 3, Panel B. This figure shows that the amount of hemoglobin measure in supernatant is the same in presence or absence of HlyA, suggesting

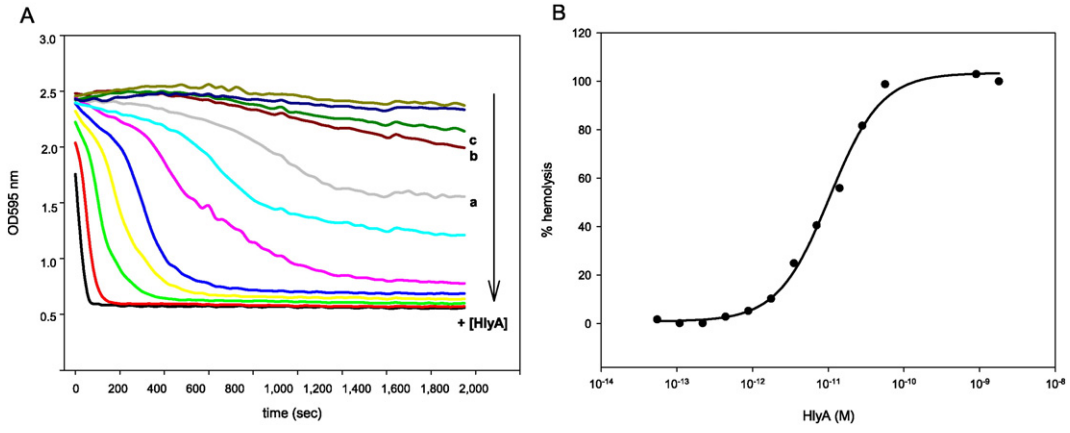

Fig. 1. Hemolytic activity of alpha-hemolysin. Panel A: hemolysis kinetics was measured as the decrease in turbidity of an erythrocyte suspension treated with increasing amounts of toxin. Curves a, b, and c correspond to 14, 7.0, and 3.5 pM alpha-hemolysin, respectively. In the figure, the absorbance of the suspension at 595 nm is plotted as a function of time of exposure to the toxin in sec on the *abscissa*. The arrow indicates the following increasing concentrations of toxin: black 1.8×10^{-9} M, red 9×10^{-10} M, light green 4.5×10^{-10} M, yellow 2.2×10^{-10} M, blue 1.1×10^{-10} M, pink 5×10^{-11} M, light blue 2.8×10^{-11} M, gray 1.4×10^{-11} M, brown 7×10^{-12} M, dark green 3.5×10^{-12} M, dark blue 1.7×10^{-12} M, and green 8.7×10^{-13} M. Panel B: this is a representative curve of three independent experiments where the percent hemolysis calculated at 30 min on the *ordinate* is expressed as a function of the molar alpha-hemolysin concentration on the *abscissa*.

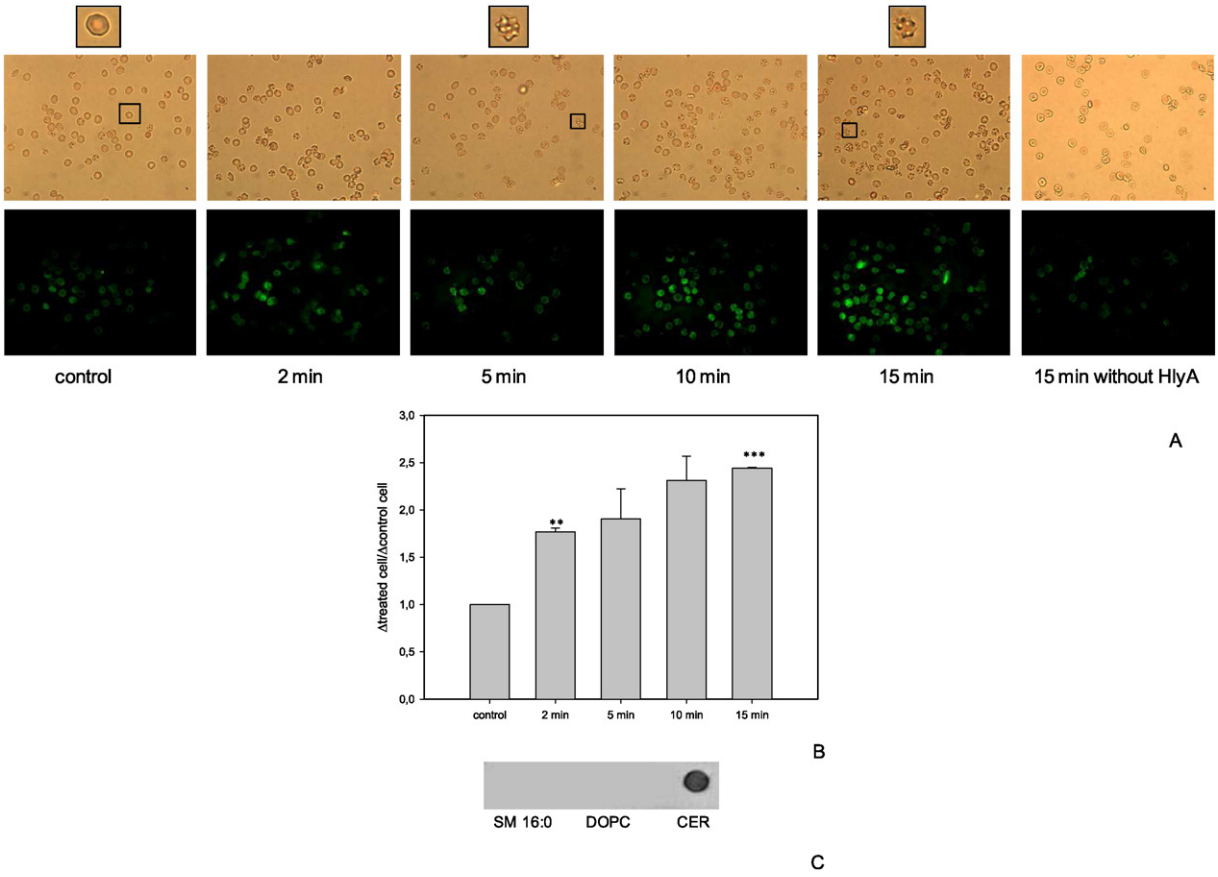

Fig. 2. Ceramide formation in erythrocytes treated with alpha-hemolysin. Erythrocytes (0.1% (v/v) were incubated with 3.5 pM of HlyA at 37 °C for 2, 5, 10 and 15 min. Samples were centrifugated at 6000 rpm, and the remaining cells were fixed with 1% (v/v) glutaraldehyde/Ringer's buffer and pelleted onto coverlips coated with 0.001% v/v poly-L-lysine. Panel A: ceramide formation on the erythrocyte-cell surface was determined by immunofluorescence. Fixed treated erythrocytes were then exposed to mouse anticeramide antibodies (1:5) followed by FITC-labeled goat anti(mouse IgG) antibodies (1:20). Both images of fluorescence and optical microscopy are shown for control and HlyA-treated erythrocytes. Images were captured with an Olympus DP70 digital camera attached to an Olympus BX51 microscope with an excitation of 460–495 nm (emission filter 510–550 nm). An objective of 100× with a NA of 1.35 was used. Panel B: captured images were analyzed using the Image J software. The fluorescence intensity of each cell was measured. The figure shows the ratio between the fluorescence intensity of each cell with the fluorescence of the background subtracted and the corresponding difference of untreated cells. Results show the fluorescence mean value of five images taken at each time of three independent experiments (**P < 0.01, ***P < 0.001). Panel C: 1.5 nmol of 1,2-dioleoyl-glycero-3-phosphocholine (DOPC), sphingomyelin (SM), and ceramide (CER) was spotted on nitrocellulose membranes. The membranes were then blocked as described in Experimental procedures section and were analyzed by immunoblotting with polyclonal anticeramide and FITC-labeled goat anti(mouse IgG) antibodies. Dot blots were developed by chemiluminescence. An equal volume was spotted for each lipid concentration assayed.

that a spontaneously hemolysis might occur due to sample manipulation during the experiment. The inset figure shows that the number of cells and the crenated ones keep constant during the experiments when HlyA is not added. This clearly demonstrates that the increment of crenated cells observed in Fig. 3 is due toxin interaction. So considering that 3.5 pM of HlyA does not produce hemolysis during 15 min, the

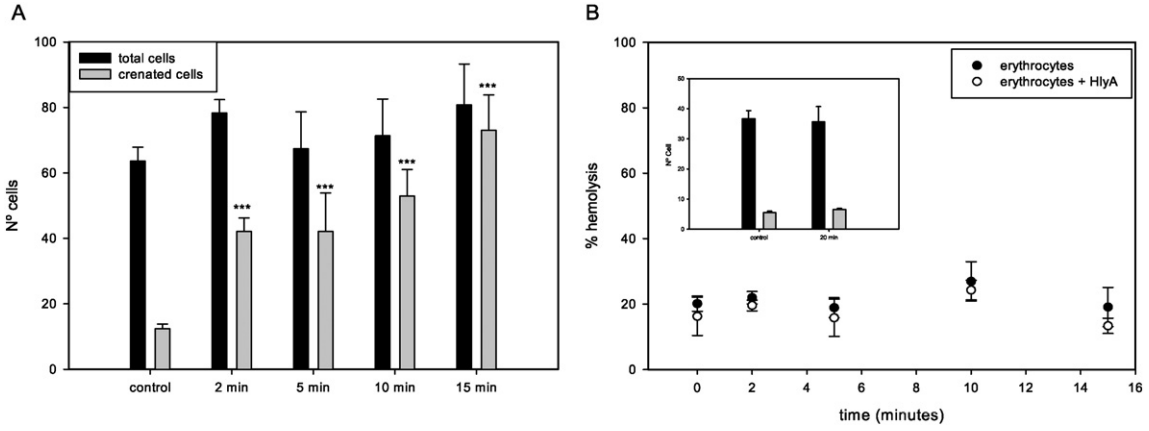

Fig. 3. Cells and hemoglobin quantification. Panel A: erythrocytes (0.1% (v/v)) were incubated with 3.5 pM of HlyA at 37 °C for 2, 5, 10 and 15 min. Samples were centrifugated at 6000 rpm, and the remaining cells were fixed with 1% (v/v) glutaraldehyde/TC buffer and pelleted onto coverlips coated with 0.001% v/v poly-L-lysine, for their quantification. Panel B: the supernatant was separated to measure hemoglobin release by spectroscopy at 412 nm. Hemoglobin release was also measured in samples of erythrocytes without HlyA treatment but that were incubated in buffer during the same period of time. Inset: Cells quantification (total and crenated cells) of untreated erythrocytes at 0 and 20 min. All results show the mean value of the counting of five images taken at each time of three independent experiments (***P < 0.001).

immunofluorescence assay for ceramide detection was performed in this condition. Fig. 2, Panel A shows the microscopy images obtained at 2, 5, 10 and 15 min. It can be seen that fluorescence intensity of the erythrocyte membranes increased considerably relative to that of the control erythrocytes. This difference is clearly shown in Fig. 2, Panel B obtained from different cells in five images captured at each time. The control assay of untreated erythrocytes at 15 min incubated with anticeramide antibody shows a very slight fluorescence (Fig. 2, panel A). On the other hand, erythrocytes treated only with goat antimouse IgG-FITC antibody lacked any fluorescence (data not shown). Fig. 2, Panel C shows that the anticeramide antibody interacted specifically with ceramide but not with either phosphatidylcholine (PC) or sphingomyelin (SM), the two main phospholipids of the outer bilayer of human erythrocytes [24]. On the basis of these results we were reassured that HlyA induced the activation of endogenous SMases with the subsequent formation of ceramide.

3.3. Calpain activation

In order to obtain a more complete understanding of the effects on erythrocytes produced by low concentrations of HlyA, we measured the calpain activity in cells treated with the toxin.

Calpains are ubiquitous calcium-dependent cysteine proteases that selectively cleave proteins in the presence of calcium. Human erythrocytes contain only calpain I (the μ-calpain), and that enzyme's activity is regulated by the endogenous inhibitor calpastatin [25].

Fig. 4 shows the calpain activity of erythrocytes treated with increased concentrations (1.8, 3.5 and 7.0 pM) of HlyA at 5 and 15 min. The calpain activity increased with time upon exposure of erythrocytes to HlyA, in a concentration-dependent manner. The differences observed in calpain activity at 15 min are significant compared to untreated erythrocytes. The reason for the slight differences observed between calpain activity at 3.5 and 7.0 pM HlyA, might be attributable to the very similar hemolysis observed at these two concentrations by 15 min., as illustrated by curves b and c of Fig. 1, Panel A. For further experiments we will use 7.0 pM of HlyA to be certain of working at sublytic levels of HlyA and be sure that calpains were activated.

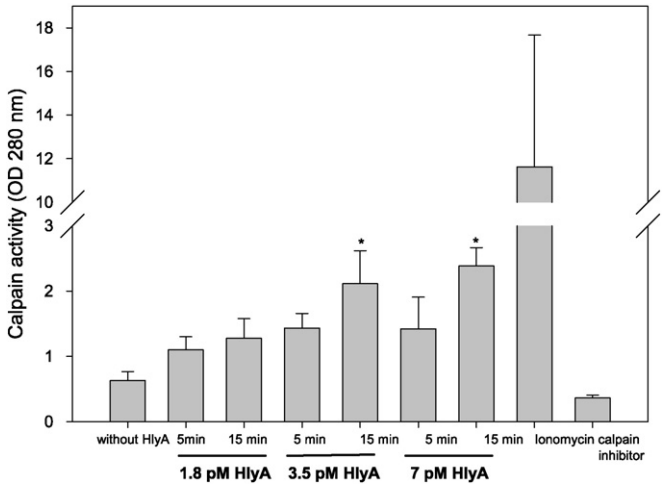

Fig. 4. Calpain activation induced by alpha-hemolysin. Calpain activity measured as the detection of trichloroacetic-acid–soluble peptide fragments from casein through absorbance at 280 nm. A suspension of 5% (v/v) erythrocytes was first preincubated with 1.8, 3.5 and 7.0 pM alpha-hemolysin for 5 and 15 min. Then the calpain activity was measured in the cell suspensions as described in Experimental procedures section. As a positive control of calpain activity, the assay was also performed on cells pretreated with 1 μM ionomycin, a calcium ionophore, for 15 min; while as a negative control the erythrocytes were incubated with the calpain inhibitor II (20 μM) before the addition of alpha-hemolysin. *$P < 0.05$. $n = 3$. In the figure, the absorbance at 280 nm is plotted for each of the experimental groups shown on the *abscissa*.

3.4. Target proteins of calpains within the erythrocyte membranes

The structural organization of the erythrocyte membrane enables it to suffer reversible deformation while maintaining its structural integrity during its 4-month period of circulation. A notable feature of those induced erythrocyte deformations is that they involve no significant change in the membrane's surface area. These unusual membrane properties are the result of the interaction between the 2-dimensional elastic network of cytoskeletal proteins with cytoplasmic domains of transmembrane proteins embedded in the plasma-membrane [26]. Transmembrane or membrane-associated proteins including the plasma-membrane Ca^{+2} pump and cytoskeletal proteins such as the electrophoretic protein bands 1, 2 (the α and β spectrins, respectively), 2.1, 3, 4.1, and 4.2 are the main targets of activated calpains [17].

Fig. 5, Panel A shows the electrophoretic profile of erythrocyte membranes treated with increasing concentrations of HlyA. A marked decrease in a protein band named B, corresponding to a MW of 90 kDa approximately, is apparent even at low concentration of HlyA (7.0 pM) and becomes less intense at the increased HlyA concentration (1 nM). A similar decrease is also observed for both bands named A. At first glance, to obtain the data for Fig. 5, Panel B we first calculated the optical density (OD) ratio between each of the two protein bands and the actin band (band C)—the latter being a protein that is not cleaved by calpain. The OD value calculated for Band A corresponded to that of both bands combined that are shown in the gel (Fig. 5, Panel A). We then expressed these respective OD ratios as a fraction value of the corresponding bands in the control sample not exposed to HlyA, with that value being set at 1.0. In the figure the data expressed in this way indicate that both bands, A and B, decreased significantly as the

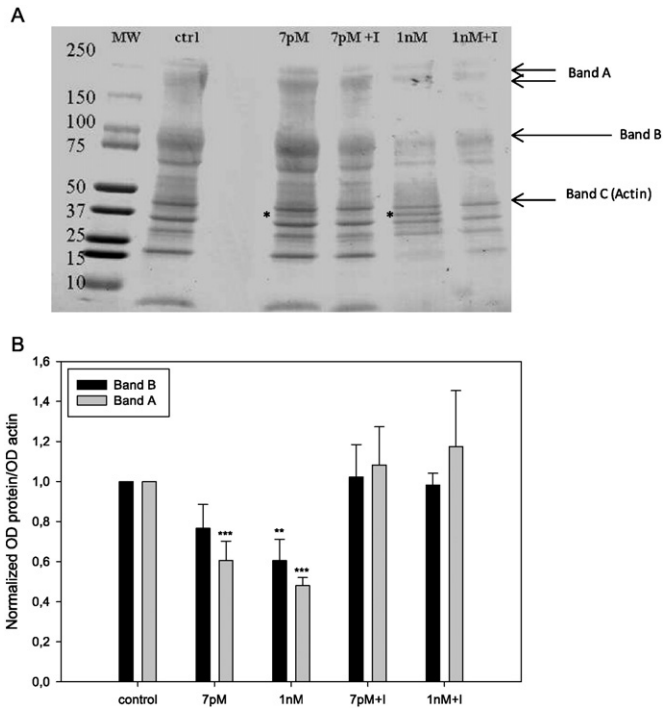

Fig. 5. Target proteins of calpains within the erythrocyte membranes. Panel A: electrophoretic profiles obtained from erythrocytes treated with alpha-hemolysin. The asterisk indicates the appearance of a band at ca. 40 kDa. Panel B: densitometric analyses were performed by the 1D Image Analysis software (ImageJ). To calculate the decrease in the Band B (black bars) and Band A (gray bars) content in alpha-hemolysin-treated erythrocytes, the optical density (OD) value corresponding to each of the two bands was expressed as a ratio relative to the OD value for the actin band. In each of 6 independent experiments ($n = 6$) the ratio of that relative value for a given protein in each of the experimental groups indicated on the *abscissa* to that of the corresponding protein in the control sample, set at a value of 1.0, was calculated and plotted on the *ordinate*. **$P < 0.01$, ***$P < 0.001$.

concentration of HlyA increased, thus confirming that the activated calpain hydrolyzes those cytoskeleton proteins. Furthermore, a band of ca. 40 kDa appeared upon HlyA treatment (Fig. 5, Panel A; asterisk).

Fig. 5, Panel A also shows the electrophoretic profile of erythrocyte membranes treated with increasing amounts of HlyA, but also in the presence of the calpain inhibitor II (lanes 4 and 6). Under this condition, the band at 40 kDa was clearly not present, and the OD ratios corresponding to Band A and B were very similar to those of the respective bands in the untreated erythrocytes (Fig. 5, Panel B). Taken together, these results provide convincing evidence that HlyA induces the activation of calpains, which in turn degrade specific cytoskeleton proteins.

To further investigate which of the cytoskeleton proteins were proteolysed by calpains, gel slices of Bands A, B, C and the band corresponding to 40 kDa (Band D) were carefully cut and analyzed on the Q Exactive™ Hybrid Quadrupole-Orbitrap (Thermo Scientific) mass spectrometer. Table 1 shows the main proteins found in bands A, B and C of control erythrocytes.

These results indicate that Band A is composed mainly by α and β spectrins, and in minor proportion of ankyrin and Band 3; Band B also contains these proteins although in smaller amounts plus Protein 4.1, and finally in Band C apart from these proteins we can find actin. The fact that Band 3 appears not only in Band B, at its expected molecular mass, but also at high proportion in Band A might be due to the presence of dimers of this protein that were not denatured by the SDS present in the loading buffer [27].

Taking profit that the peptide spectrum matches parameter (PSM), a scoring function that measures the "matching" quality between a spectrum and a peptide, is proportional to the amount of peptides identified for a certain hit and therefore proportional to the amount of protein in the studied sample, we summarize in Table 2 the PSM found for each hit in each band in control and treated-erythrocytes with 7 and 1 nM of HlyA.

From the analysis of data presented in Table 2 we can observe that α, β spectrins and ankyrin-1 are mainly concentrated in Band A and that their amount decreases significantly upon 1 nM HlyA treatment. Additionally, it can be seen that in erythrocytes treated with 7 pM of HlyA, a great amount of these protein is found in Band C (highlighted numbers). Taking into account that Band C comes from a molecular mass range of around 40 kDa, the increment of PSM for these proteins at this MW can only be explained by their proteolysis. The same effect is observed for protein 4.1, with the difference that this protein is concentrated in Band B in the control experiment. On the other hand, it is difficult to assign the presence of Band 3 in Band A or B, but if we consider the MW of the monomer we can propose that Band 3 is concentrated in Band B. In this case we can also observe a decrease in its amount with HlyA concentration, and the increment of fragmented peptides of this protein in Band C. Instead, actin, which is concentrated in Band C, does not decrease significantly with HlyA treatment as the other proteins. It is import to mention that actin in erythrocytes treated with 7 pM of HlyA is distributed between B and C, probably due to technical reasons of the way the band was cut from the gel. The decrease of proteins amount is shown in Fig. 6.

Table 2
The PSM of each protein in the bands studied in control and HlyA-treated erythrocytes.

	Band A	Band B	Band C
α-Spectrin			
0 pM HlyA	560	218	81
7 pM HlyA	630	152	**511**
1 nM HlyA	248	20	40
β-Spectrin			
0 pM HlyA	490	181	90
7 pM HlyA	586	112	**469**
1 nM HlyA	190	18	25
Ankyrin-1			
0 pM HlyA	271	79	35
7 pM HlyA	313	56	**246**
1 nM HlyA	59	4	19
Band 3			
0 pM HlyA	166	167	68
7 pM HlyA	294	103	**379**
1 nM HlyA	76	53	21
Protein 4.1			
0 pM HlyA	16	79	35
7 pM HlyA	39	45	**195**
1 nM HlyA	0	0	15
Actin			
0 pM HlyA	5	6	83
7 pM HlyA	8	36	11
1 nM HlyA	0	0	72

Bold numbers indicate the increment of fragmented peptides of each protein in Band C.

Table 3 shows the proteins found in Band D, the band which is made apparent in the gel at around 40 kDa only upon HlyA treatment (Fig. 5, Panel A).

The PSM for each protein shows that at 7 pM of HlyA in at around 40 kDa (Band D) there is a coelution of fragments of α and β spectrins, ankyrin, prot 4.1 and Band 3, with actin; but when erythrocytes are treated with lytic concentration of HlyA, only fragments of Band 3 are found in this band.

The data used for the analysis presented can be seen in the Supplementary files SF1, SF2, SF3 and SF4, corresponding to Band A, B, C and D analysis, respectively.

On the basis of these results, we can conclude that at low concentration (7 pM) HlyA activates calpains that degradates α and β spectrins,

Table 1
Protein identification in each studied band.

Band	Accession no.	Description	Score	MW (kDa)
A	P02549	Spectrin alpha chain, erythrocytic 1 OS = *Homo sapiens*	1511.46	279.8
	P11277	Spectrin beta chain, erythrocytic OS = *Homo sapiens*	1285.04	246.3
	P16157-16	Isoform Er15 of Ankyrin-1 OS = *Homo sapiens*	702.56	203.3
	P02730	Band 3 anion transport protein OS = *Homo sapiens*	378.13	101.7
B	P02549	Spectrin alpha chain, erythrocytic 1 OS = *Homo sapiens*	517.03	279.8
	P11277	Spectrin beta chain, erythrocytic OS = *Homo sapiens*	443.88	246.3
	P02730	Band 3 anion transport protein OS = *Homo sapiens*	320.81	101.7
	P16157-10	Isoform Er3 of Ankyrin-1 OS = *Homo sapiens*	186.43	197.6
	P11171-3	Isoform 3 of Protein 4.1 OS = *Homo sapiens*	188.48	93.2
C	P02549	Spectrin alpha chain, erythrocytic 1 OS = *Homo sapiens*	175.90	279.8
	P11277	Spectrin beta chain, erythrocytic OS = *Homo sapiens*	179.40	246.3
	P02730	Band 3 anion transport protein OS = *Homo sapiens*	115.91	101.7
	P60709	Actin, cytoplasmic 1 OS = *Homo sapiens*	183.09	41.7

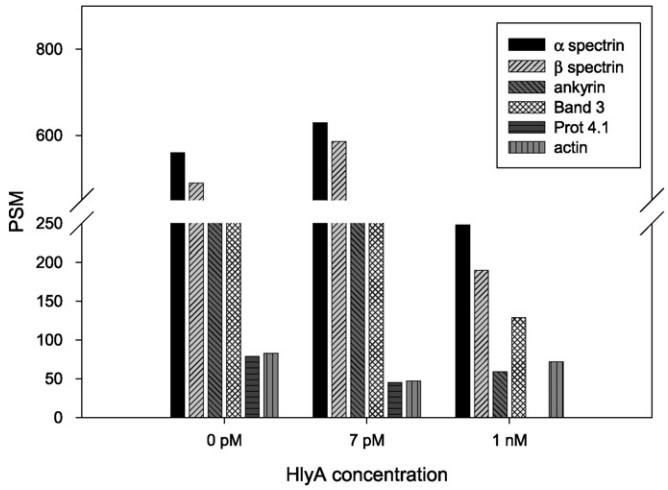

Fig. 6. PSM of each protein. The PSM of α and β spectrin, ankyrin, band 3, prot 4.1 and actin was graphed for control and treated erythrocytes with 7 and 1 nM of HlyA.

ankyrin, prot 4.1 and Band 3, generating peptides of 40 kDa approximately, but at higher toxin concentration the peptides generated are smaller.

4. Discussion

Uropathogenic *E. coli* strains find an extremely nutrient-poor host environment; that was the reason why it was primarily thought that the function of HlyA was to lyse host cells, thereby facilitating the release of nutrients and other substances that are critical for bacterial growth. Nevertheless, what is not clear is how often HlyA reaches levels that are high enough to lyse host target cells during the course of an infection. In fact, sublytic concentrations of HlyA may be even more physiologically relevant within such a scenario. Indeed, recent studies have demonstrated that sublytic concentrations of a number of pore-forming toxins can modulate a variety of host signaling pathways; including the transient stimulation of calcium oscillations, an activation of the mitogen-activated-protein-kinase signaling, and an alteration of the histone-phosphorylation and -acetylation patterns [28,29]. In addition, sublytic concentrations of HlyA have been recently found to potently stimulate the inactivation of protein kinase B, a key enzyme in host cell-cycle progression, metabolism, vesicular trafficking, survival, and inflammatory-signaling pathways [30]. In this work we further investigated the effects induced by low concentrations of HlyA in erythrocytes, the major cell type present in blood.

We observed that the hemolysis increased with elevated HlyA concentrations (Fig. 1, Panel B), while the kinetics of the process also changed at progressively higher levels of the toxin (Fig. 1, Panel A). At HlyA concentrations higher than the D_{50}, changes in the OD with time display a cooperative behavior, with a short lag period occurring before erythrocyte hemolysis. This interval diminished as the toxin concentration increased. At toxin concentrations below the D_{50} (i.e., 9.5 pM), however, this cooperativity disappeared and the OD diminished directly and linearly with time (Fig. 1, Panel A). This shift indicated that the mechanism of erythrocyte lysis at high and low levels of toxin is different. The cooperativity at high toxin concentration has been associated with an oligomeric pore formation [31,32]. These observations raised the question as to what happens in erythrocytes interacting with toxin concentrations that are low because of dilution in the blood and whether or not such erythrocytes would lyse in the same way.

In order to answer these questions, we studied the effects induced by low concentrations of HlyA in erythrocytes as a simulation of the dilute situation within the circulation. Recently, López et al. have demonstrated that SMase activity increases because of an increment in the membrane-bending energy [33]. This observation prompted us to study the possibility of an activation of SMase resulting from changes in the membrane-bending energy subsequent to an insertion of the toxin into the membrane. Whether erythrocytes contain a neutral [33] or an acid [21] SMase is still not clear; but both enzymes catalyze the production of ceramide from the SM present in the outer layer of the membrane, with the difference in their action being only the pH optimum for catalysis [34]. Figs. 2 and 3 illustrate that the ceramide concentration increases in erythrocytes treated with a low concentration of toxin after 15 min. Ceramide is a sphingolipid that has gained much attention as a key signaling molecule in vital cell processes—e.g., eryptosis [21]. This role is mainly attributable to the ceramide chemical structure, whose geometry induces changes in the biophysical properties of membranes. The tight cohesive interactions between ceramide molecules leads phase separation of ceramide-rich and -poor microdomains [35], thus generating defects in the interfaces. This form of interaction might explain the lag phase and gradual hemolysis observed at low concentrations of HlyA (Fig. 1).

In a previous publication we demonstrated that the intracellular calcium concentration increased from 60 nM up to 150 nM before the onset of hemolysis when erythrocytes had been in contact with the toxin [10]. Since calpains ubiquitously are calcium-dependent cysteine proteases that selectively cleave proteins in response to calcium, we were prompted to study the activation of these proteases within the context of the action of HlyA. Human erythrocytes contain only calpain I (the μ-calpain), whose activity is regulated by the endogenous inhibitor calpastatin [25]. Fig. 4 demonstrates that calpain activity increases when erythrocytes are treated with an extremely low HlyA concentration (3.5 pM). Although mature erythrocytes contain caspases, those enzymes were seen to remain inactive, with calpains being the proteases that were activated in response to elevated calcium levels [15] to further induce events precipitating eryptosis—namely the proteolysis of membrane and transmembrane proteins, such as spectrins, ankyrin, Band 3 and protein 4.1 (Figs. 5 and 6), so as to modify the erythrocyte shape and produce cell shrinkage. HlyA-treated erythrocytes exhibit a reduction of these proteins levels and a putative cleavage product of the latter at 40 kDa (Fig. 6). This band is not visible in the presence of the calpain inhibitor II, thus confirming that HlyA induces authentic calpain activation. Furthermore, De Franceschi et al. suggested that calpain I is involved in enhancing Gardos-channel activity [36]. Accordingly, because calpain I modulates the activity of the membrane-transport systems involved in the regulation of erythrocyte hydration and therefore shape, we can state that the shrinkage of erythrocytes treated with HlyA that was both observed by Skals et al. [9] and demonstrated in these present experiments (Fig. 3) was caused by the activation of calpains and that the proteolysis by these enzymes activated the Gardos channel to destabilize the erythrocyte cytoskeleton. Berg et al. demonstrated that the calpain inhibitor prevented spectrin degradation by calpain, as we have likewise shown in this work (Fig. 5, Panel B), and also forestalled erythrocyte shrinkage; but the exposure of PS remained unaffected [15]. Thus the exposure of this phospholipid in erythrocytes treated with HlyA [9] might result from a flip-flop lipid movement

Table 3
The PSM of each protein in Band D in control and HlyA-treated erythrocytes.

	Band D		Band D
α-Spectrin		Band 3	
7 pM HlyA	77	7 pM HlyA	30
1 nM HlyA	0	1 nM HlyA	7
β-Spectrin		Protein 4.1	
7 pM HlyA	69	7 pM HlyA	11
1 nM HlyA	0	1 nM HlyA	0
Ankyrin-1		Actin	
7 pM HlyA	41	7 pM HlyA	55
1 nM HlyA	0	1 nM HlyA	0

produced by an increase in ceramide through the enzymatic activation of SMase [33] that in turn was caused by an HlyA-induced increment in membrane-bending energy.

The normal biconcave human erythrocyte possesses a 40% greater surface area than a sphere of the same volume (90 fL), giving the cell the property to deform. The maintenance of erythrocyte shape is mediated by a strong cohesion between the bilayer and the membrane skeleton, preventing membrane vesiculation and membrane breakup. Of the various linkages that have been documented, those mediated by Band 3 appear to be the dominant determinants of that membrane cohesiveness [26]. This role of Band 3 might explain the change in erythrocyte shape upon HlyA treatment (Fig. 2). We observed that the activation of calpains induced the proteolyses of Band 3 (Fig. 5), and that cleavage might favor the formation of microvesicles that, in turn, produce a reduction in erythrocyte volume. The increase in ceramide in the membrane also facilitates the budding of vesicles [37], though that phenomenon needs to be further investigated.

In view of all these results together, we can conclude that at low toxin concentrations erythrocytes undergo a series of biochemical and morphologic changes provoked by a calcium influx that induces a

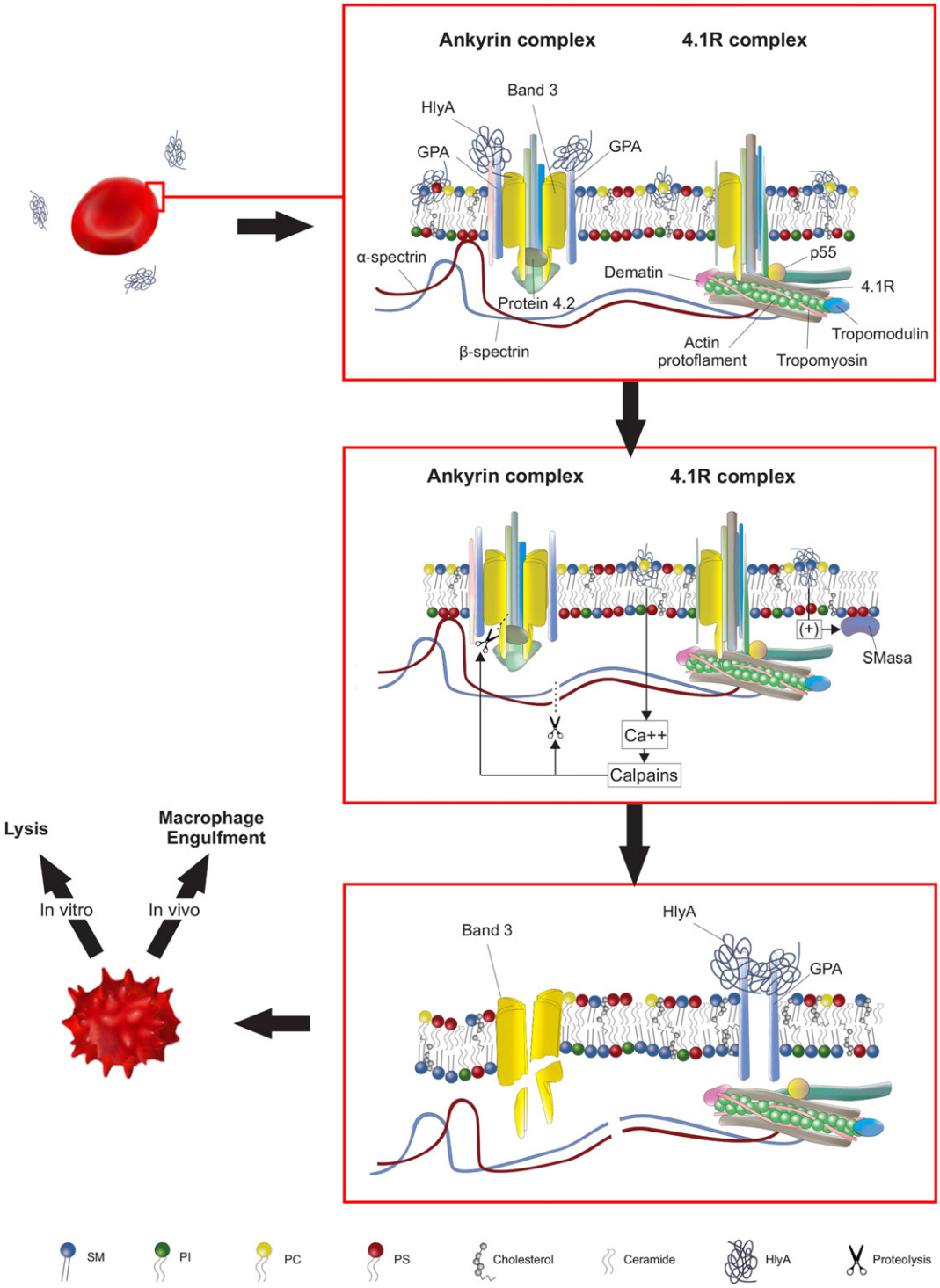

Fig. 7. Summary of the effect produced by a low concentration of alpha-hemolysin.

proteolytic activation of calpain. Moreover, the mechanical stress produced by the insertion of the toxin into the membrane activates SMase with a consequent modification of the membrane-lipid composition that, for its part, participates in a synergic effect on the structure and properties of the membrane. Both calcium and ceramide are second messengers in the induction of eryptosis. Thus, through this concatenation of effects, HlyA at low concentrations induces the eryptosis of damaged erythrocytes in vivo, as summarized in the model depicted in Fig. 7. In this figure glycophorin A (GPA) was introduced because it was characterized as receptor for HlyA in erythrocytes [38]. Further investigation is needed to clarify if its interaction with the toxin might affect its participation in the complex of attachment of the membrane to the cytoskeleton. In vivo, suicidal erythrocyte death accomplishes the clearance of defective red cells before hemolysis. The presence of PS on the erythrocyte surface promotes the adherence of eryptotic cells to the endothelial elements and also promotes erythrocyte phagocytosis and intracellular degradation by macrophages. In contrast, in vitro, the biophysical changes in the erythrocyte membrane at low toxin concentrations result in only a gradual hemolysis.

Unlike with other pore-forming toxins, the putative pores formed by HlyA and related toxins have still not been observed—not even by electron microscopy, crystal-structure determination, atomic-force microscopy, or other imaging techniques. That despite the high molecular mass of this toxin the direct visualization of such a pore has not yet been possible is indeed remarkable. Rather, the pore-forming capacity of HlyA has always been determined indirectly by osmotic protection and electrophysiological experiments [4,39–41]. Perhaps such a pore-like structure does not exist and the cytolytic effects observed result from several signals triggered by the interaction of HlyA with the membrane.

This figure shows a summary of the results present in this manuscript. The first panel shows the structure of the main complexes (ankyrin and 4.1R complexes) involve in the interaction between the membrane and the cytoskeleton network. Our results demonstrate that low toxin concentrations induce a series of biochemical and morphologic changes of erythrocytes provoked by a calcium influx that induces a proteolytic activation of calpain. Moreover, the mechanical stress produced by the insertion of the toxin into the membrane activates SMase with a consequent modification of the membrane-lipid composition that, for its part, participates in a synergic effect on the structure and properties of the membrane (mid panel). Both calcium and ceramide are second messengers in the induction of eryptosis (last panel). Thus, through this concatenation of effects, HlyA at low concentrations induces the eryptosis of damaged erythrocytes in vivo, which accomplishes the clearance of defective red cells before hemolysis. In contrast, in vitro, the biophysical changes in the erythrocyte membrane at low toxin concentrations result in only a gradual hemolysis.

5. Concluding remarks

In the present work we demonstrate that in human erythrocytes HlyA induces activations of both endogenous calpains and SMases to effect morphologic changes that result from both a destabilization of the cytoskeleton and a cleavage of proteins involved in the regulation of the erythrocyte volume and shape. These alterations precipitate the eryptosis of damaged erythrocytes. By this means eryptosis can function as a useful mechanism to remove defective erythrocytes before hemolysis. Nevertheless, excessive eryptosis can lead to anemia—if an accelerated eryptosis cannot be compensated by a corresponding increase in erythropoeisis—and thus diminish microcirculation, through the adherence of PS-exposed erythrocytes to the vascular wall. In addition, since erythrocytes with exposed PS also stimulate blood clotting [42], excessive eryptosis could also lead to thrombosis.

Supplementary data to this article can be found online at http://dx.doi.org/10.1016/j.bbamem.2015.08.012.

Funding

This work was supported by the Agencia Nacional de Promoción Científica y Tecnológica [grant number PICT 2011/551] and the Universidad Nacional de La Plata [grant number M/164].

Author contributions

FC and VH performed all the experiments. SM, LB, and VH planned the experiments, analyzed the experimental data, and wrote the paper.

Acknowledgments

L.B. and S.M. are members of the Carrera del Investigador Comisión de Investigaciones Científicas de la Provincia de Buenos Aires (CICBA), Argentina. V.H. is a member of the Carrera del Investigador of Consejo Nacional de Investigación en Ciencia y Tecnología (CONICET). S.M., L.B. and V.H. are members of the Iberoamerican CYTED Network BIOTOX 212RT0467. Dr. Donald F. Haggerty, a retired career investigator and native English speaker, edited the final version of the manuscript. The authors thank Dra. Silvia Moreno for her help in the mass spectrometric analysis.

References

[1] S. Cavalieri, G.A. Bohach, I. Synder, *Escherichia coli* α-hemolysin characteristics and probable role in pathogenicity, Microbiol. Rev. 48 (1984) 326–343.
[2] D.J.J. Evans, D.G. Evans, C. Höhne, M.A. Noble, E.V. Haldane, H. Lior, L.S. Young, Hemolysin and K antigens in relation to serotype and hemagglutination type of *Escherichia coli* isolated from extraintestinal infections, J. Clin. Microbiol. 13 (1) (1981) 171–178.
[3] S. Bhadki, H. Bailey, A. Valava, I. Walev, B. Walker, U. Weller, M. Kehoe, M. Palmer, Staphylococcal alpha-toxin, streptolysin-O, and *Escherichia coli* hemolysin: prototype of pore-forming bacterial cytolisins, Arch. Microbiol. 165 (1996) 73–79.
[4] S. Bhakdi, N. Mackman, J.M. Nicaud, I. Holland, *Escherichia coli* hemolysin may damage target cell membranes by generating transmembrane pores, Infect. Immun. 52 (1986) 63–69.
[5] A. Laestadius, A. Richter-Dahlfors, A. Aper, Dual effects of *Escherichia coli* α-hemolysin on rat renal proximal tubule cells, Kidney Int. 62 (2002) 2035–2042.
[6] P. Uhlen, A. Laestadius, T. Jahnukainen, T. Soderblom, F. Backhed, G. Celsi, H. Brisman, S. Normark, A. Aperia, A. Richter-Dahlfors, Alpha-haemolysin of uropathogenic *E. coli* induces Ca^{2+} oscillations in renal epithelial cells, Nature 405 (2000) 694–697.
[7] A. Koschinski, H. Repp, H. Unver, F. Dreyer, D. Brockmeier, A. Valeva, S. Bhakdi, I. Walev, Why *Escherichia coli* α-hemolysin induces calcium oscillations in mammalian cells—the pore is on its own, FASEB J. (2006) E80–E87.
[8] M. Skals, N.R. Jorgensen, J. Leipziger, H.A. Praetorius, Alpha-hemolysin from *Escherichia coli* uses endogenous amplification through P_2X receptor activation to induce hemolysis, Proc. Natl. Acad. Sci. U. S. A. 106 (10) (2009) 4030–4035.
[9] M. Skals, U. Jensen, J. Ousingsawat, K. Kunzelmann, J. Leipziger, H. Praetorius, *Escherichia coli* alpha-hemolysin triggers shrinkage of erythrocytes via K(Ca)3.1 and TMEM16A channels with subsequent phosphatidylserine exposure, J. Biol. Chem. 285 (20) (2010) 15557–15565.
[10] S. Sanchez, L. Bakás, E. Gratton, V. Herlax, Alpha hemolysin induces an increase of erythrocytes calcium: a FLIM 2-photon phasor analysis approach, PLoS One 6 (6) (2011) e21127.
[11] M. Skals, H.A. Praetorius, Mechanisms of cytolysin-induced cell damage — a role for auto- and paracrine signalling, Acta Physiol (Oxf). 209 (2) (2013) 95–113.
[12] M. Foller, S.M. Huber, F. Lang, Erythrocyte programmed cell death, Life 60 (10) (2008) 661–668.
[13] T. Murachi, Calcium-dependent proteinases and specific inhibitors: calpain and calpastatin, Biochem. Soc. Symp. 49 (1984) 149–167.
[14] T. Glaser, N. Schwarz-Benmeir, S. Barnoy, S. Barak, Z. Eshhar, N.S. Kosower, Calpain (Ca(2+)-dependent thiol protease) in erythrocytes of young and old individuals, Proc. Natl. Acad. Sci. U. S. A. 16 (1994) 7879–7883.
[15] C.P. Berg, I.H. Engels, A. Rothbart, K. Lauber, A. Renz, S.F. Schlosser, K. Schulze-Osthoff, S. Wesselborg, Human mature red blood cells express caspase-3 and caspase-8, but are devoid of mitochondrial regulators of apoptosis, Cell Death Differ. 8 (12) (2001) 1197–1206.
[16] D.E. Goll, V.F. Thompson, H. Li, W. Wei, J. Cong, The calpain system, Physiol. Rev. 83 (3) (2003) 731–801.
[17] A. Bogdanova, A. Makhro, J. Wang, P. Lipp, L. Kaestner, Calcium in red blood cells — a perilous balance, Int. J. Mol. Sci. 14 (5) (2013) 9848–9872.
[18] M. Moayeri, R. Welch, Prelytic and lytic conformation of erythrocyte-associated *Escherichia coli* hemolysin, Infect. Immun. 65 (6) (1997) 2233–2239.

[19] K. Wang, P. Yeun, K. Lee, Calpain in excitotoxicity, cerebral ischemia, and neuronal apoptosis, in: K. Wang, P. Yeun (Eds.), Calpain: Pharmacology and Toxicity of Calcium-dependent Proteases, Taylor and Francis, USA 1999, pp. 179–190.
[20] M. Bradford, A rapid and sensitive method for quantification of microgram quantities of protein utilizing the principle of protein dye binding, Anal. Biochem. 72 (1976) 248–254.
[21] K.S. Lang, S. Myssina, S. Brand, C. Sandu, P.A. Lang, S. Berchtold, S.M. Huber, F. Lang, T. Wieder, Involvement of ceramide in hyperosmotic shock induced death of erythrocytes, Cell Death Differ. 11 (2004) 231–243.
[22] K.S. Lang, P.A. Lang, C. Bauer, C. Duranton, T. Wieder, S.M. Huber, F. Lang, Mechanisms of suicidal erythrocyte death, Cell. Physiol. Biochem. 15 (2005) 195–202.
[23] K.S. Lang, C. Duranton, H. Poehlmann, S. Myssina, C. Bauer, F. Lang, T. Wieder, S.M. Huber, Cation channels trigger apoptotic death of erythrocytes, Cell Death Differ. 10 (2) (2003) 249–256.
[24] K.S. Koumanov, C. Tessier, A.B. Momchilova, D. Rainteau, C. Wolf, P.J. Quinn, Comparative lipid analysis and structure of detergent-resistant membrane raft fractions isolated from human and ruminant erythrocytes, Arch. Biochem. Biophys. 434 (1) (2005) 150–158.
[25] D.E. Goll, V. Thompson, H. LI, W. Wei, J. Cong, The calpain system, Physiol. Rev. 83 (2003) 731–801.
[26] N. Mohandas, P.G. Gallagher, Red cell membrane: past, present, and future, Blood 112 (10) (2008) 3939–3948.
[27] R.C. Williamson, A.M. Toye, Glycophorin A: band 3 aid, Blood Cell Mol. Dis. 41 (2008) 35–43.
[28] M.A. Hamon, E. Batsche, B. Regnault, T.N. Tham, S. Seveau, C. Muchardt, P. Cossart, Histone modifications induced by a family of bacterial toxins, Proc. Natl. Acad. Sci. U. S. A. 104 (33) (2007) 13467–13472.
[29] A.J. Ratner, K.R. Hippe, J.L. Aguilar, M.H. Bender, A.L. Nelson, J.N. Weiser, Epithelial cells are sensitive detectors of bacterial pore-forming toxins, J. Biol. Chem. 281 (18) (2006) 12994–12998.
[30] T.J. Wiles, B.K.-. Dhakal, D.S. Eto, M.A. Mulvey, Inactivation of host Akt/protein kinase B signalling by bacterial pore-forming toxins, Mol. Biol. Cell 19 (2008) 1427–1438.
[31] V. Herlax, S. Maté, O. Rimoldi, Relevance of fatty acid covalently bound to *Escherichia coli* α-hemolysin and membrane microdomains in the oligomerization process, J. Biol. Chem. 284 (2009) 25199–25210.
[32] V. Herlax, M.F. Henning, A.M. Bernasconi, F.M. Goni, L. Bakas, The lytic mechanism of *Escherichia coli* α-hemolysin associated to outer membrane vesicles, Health 2 (2010) 484–492.
[33] D. López, M. Egido-Gabas, I. López-Montero, J.V. Busto, J. Casas, M. Garnier, F. Monroy, B. Larijani, F. Goñi, A. Alonso, Accumulated bending energy elicits neutral sphingomyelinase activity in human red blood cells, Biophys. J. 102 (2012) 2077–2085.
[34] F. Goñi, A. Alonso, Sphingomyelinases: enzymology and membrane activity, FEBS Lett. 531 (2002) 38–46.
[35] R.N. Kolesnick, F.M. Goni, A. Alonso, Compartmentalization of ceramide signaling: physical foundations and biological effects, J. Cell. Physiol. 184 (3) (2000) 285–300.
[36] L. De Franceschi, R.S. Franco, M. Bertoldi, C. Brugnara, A. Matte, A. Siciliano, A.J. Wieschhaus, A.H. Chishti, C.H. Joiner, Pharmacological inhibition of calpain-1 prevents red cell dehydration and reduces Gardos channel activity in a mouse model of sickle cell disease, FASEB J. 27 (2) (2013) 750–759.
[37] A.E. Cremesti, F.M. Goni, R. Kolesnick, Role of sphingomyelinase and ceramide in modulating rafts: do biophysical properties determine biologic outcome? FEBS Lett. 531 (1) (2002) 47–53.
[38] A. Cortajarena, F. Goñi, H. Ostolaza, Glycophorin as a receptor for *Escherichia coli* α-hemolysin in erythrocytes, J. Biol. Chem. 276 (16) (2001) 12513–12519.
[39] M. Moayeri, R. Welch, Effects of temperature, time, and toxin concentration on lesion formation by the *Escherichia coli* hemolysin, Infect. Immun. 62 (10) (1994) 4124–4134.
[40] G. Menestrina, N. Mackman, I.B. Holland, S. Bhadki, *Escherichia coli* haemolysin forms voltage-dependent ion channels in lipid membranes, Biochem. Biophys. Acta 905 (1987) 109–117.
[41] L. Bakás, A. Chanturiya, V. Herlax, J. Zimmerberg, Paradoxical lipid dependence of pores formed by *Escherichia coli* α-hemolysin in planar phospholipids bilayer membranes, Biophys. J. 91 (10) (2006) 3748–3755.
[42] S.M. Chung, O.N. Bae, K.M. Lim, J.Y. Noh, M.Y. Lee, Y.S. Jung, J.H. Chung, Lysophosphatidic acid induces thrombogenic activity through phosphatidylserine exposure and procoagulant microvesicle generation in human erythrocytes, Arterioscler. Thromb. Vasc. Biol. 27 (2007) 414–421.